SI Appendix

Manuscript: Molecular requirements for a pandemic influenza virus: an acid-stable hemagglutinin protein

Authors: Marion Russier, Guohua Yang, Jerold E. Rehg, Sook-San Wong, Heba H. Mostafa, Thomas P. Fabrizio, Subrata Barman, Scott Krauss, Robert G. Webster, Richard J. Webby, Charles J. Russell

SI Methods

Cells and Viruses. MDCK, A549, and Vero cells were maintained in Dulbecco's modified Eagle's medium (DMEM) supplemented with 5% fetal bovine serum (FBS). BHK cells were maintained in DMEM with 10% FBS. NHBE cells (Lonza) were maintained and differentiated as described (1). A/Tennessee/1-560/2009 recombinant viruses were generated as described and propagated in MDCK cells (2). Infectious titers were determined by plaque assay in MDCK cells. Sanger sequencing confirmed virus identity and absence of unintended mutations. Swine and human influenza viruses obtained from the St. Jude repository (Table S1) were isolated in 10-day-old embryonated eggs and propagated in MDCK cells if needed.

Animal Experiments. Six-week-old female DBA/2J mice (Jackson Laboratories, Bar Harbor, ME) were anesthetized with isoflurane and intranasally inoculated with 750 PFU of virus in 30 µL PBS. On days 3, 5, 7, and 10, mice were euthanized with $C0_2$ and the lungs, trachea, and nasal cavity were collected. 5-month-old male ferrets (Triple F farms) seronegative for influenza A viruses were anesthetized with isoflurane and inoculated intranasally with 10^6 PFU in 0.5 ml PBS. Naive ferrets were introduced the following day for contact- and airborne-transmission experiments. Clinical signs, temperature, and weight were recorded daily. Every other day, nasal washes were collected. On day 3 and 6 after inoculation, ferret tissue from the trachea and each lobe of the lungs was collected for virus titration and mRNA analysis. Organs or tissue were homogenized in PBS in the Qiagen Tissue Lyser II. Virus in the supernatants of centrifuged homogenates was titrated by $TCID_{50}$ in MDCK cells.

Gene Sequencing. Sanger and next generation sequencing were used to determine amino-acid residue variations for ferret nasal wash samples. Sanger sequencing was performed on the complete gene segments of HA, NA, and M. Next generation sequencing was performed on the complete HA gene segment. Full-length HA genes were amplified using One-Step RT-PCR Kit (Qiagen) and H1-specific primers 5′-tgtaaaacggccagtatgaaggcaatactagtag-3′ and 5′-caggaaacagctatgaccaatacatattctacactgtagagaccca-3′. A few samples required the amplification of 2 HA segments using additional primers (5'-tgtaaaacgacggccagtgattgcaatacaacttgtc-3' and 5'-caggaaacagctatgaccgatcggatgtatattctgaaatgg-3'). PCR amplicons were purified by QIAquick gel extraction kit (Qiagen) and prepared using Nextera XT cDNA library preparation kit (Illumina) according to the manufacturer's protocol. High-throughput paired-end sequencing was done using a 2 x 150 bp cycle on an Illumina MiSeq platform. Data analysis was done using CLC Genomics Workbench 8 (CLC Bio). Briefly, reads were aligned to the sequence of the wild-type virus, and the mapped reads were put through the Quality-Based Variant Detection pipeline. The variants were called if they met the predefined quality scores and present in both forward and reverse reads at equal ratios. In addition, the minimum variant read frequency was set at 5%, and variants had to be supported by a minimum of 10 reads. The full HA segment was completely and equally covered for all the samples. The approximate mean sequencing coverage value for the called variants identified within the amplicons was 9,460 (± 3,761 SD).

HA Acid Stability. HA activation pH was measured by syncytia assay (3). 24 h after infection, HA-expressing BHK or Vero cells were incubated for 5 min with TPCK-treated trypsin and pH-adjusted PBS buffers, then neutralized and incubated in regular medium for 3 h at 37°C. Cells were then fixed and stained for microscopy. To measure the effect of acid exposure on *in vitro* inactivation, virus stocks were incubated 1h at 37°C in pH-adjusted PBS solutions before neutralization and $TCID_{50}$ determination in MDCK cells.

HA Expression and Cleavage. Total and surface expression of HA *in vitro* was measured as previously described (4, 5). Briefly, the HA and NA genes of pH1N1 (WT or Y17H) were subcloned into pCAGGS expression vector. Vero cells were transfected with 1μg pCAGGS-HA and 0.1μg pCAGGS-NA plasmids by using a Lipofectamine Plus expression system (Invitrogen). The cells were incubated for 24 h at 37°C to allow expression of the HA and NA proteins. To detect HA cleavage, cells were treated with 5μg/ml TPCK-treated trypsin for 15 min and lysed with radioimmunoprecipitation (RIPA) buffer containing protease inhibitors. Lysates were electrophoresed on 4% to 12% NuPAGE Bis-Tris polyacrylamide-SDS gels (Invitrogen), transferred to PVDF membranes, and treated with polyclonal anti-HA goat antiserum (G618, NR15696, BEI Resources, NIAID, NIH). Protein bands were visualized using horseradish peroxidase-conjugated anti-goat antibody.

Receptor-Binding Specificity Assay. We used a solid-phase binding assay to measure the specificity of the HA protein for binding to host α2,3-linked vs. α2,6-linked sialic acid receptors. Plates were coated with 10μg/ml fetuin (Sigma). 128 HA units of sucrose-purified virus were then added to the wells. Plates were incubated overnight at 4°C to allow binding of the virus and then washed with PBS and incubated for 1 h at 4°C with PBS containing 0.1% bovine serum albumin (Sigma) desialyated by treatment with *Vibrio cholera* neuraminidase. Plates were washed with cold PBS containing 0.01% Tween-80 and incubated with serial dilutions of biotinylated sialylglycopolymers (3'sialyllactose/3'SL: Neu5Acα2-3Galβ1-4Glc and 6'sialyllactosamine/6'SLN: Neu5Acα2-6Galβ1-4Glcβ;

Glycotech) for 1.5 h at 4°C. After washing, plates were incubated with horseradish peroxidase-conjugated streptavidin (Invitrogen) diluted 1:500, for 1 h at 4°C. Plates were then washed and finally incubated with tetramethylbenzidine substrate (Thermo Scientific), and the optical density was measured at 450 nm. As a control, we used recombinant avian-like A/Puerto Rico/8/1934 virus expressing the HA of A/Mallard/Alberta/383/2009 H5N1, which has α2,3-sialic acid binding specificity.

Virus Growth. To study multiple-step growth kinetics, confluent monolayers of MDCK, A549, and NHBE cells were infected with a multiplicity of infection (MOI) of 0.01 PFU/cell. Supernatants were collected at indicated time points, stored at −80°C, and titrated in MDCK cells by 50% tissue culture infective dose ($TCID_{50}$) assay as described by (6).

Histology and Immunochemistry. Mice and ferrets (3 per group) were euthanized by CO_2 or by exsanguination under deep anesthesia, respectively. Whole lungs, tracheas, and nasal turbinates were fixed in 10% neutral buffered formalin, embedded in paraffin, and sliced. Slides were stained with hematoxylin and eosin or with polyclonal anti–influenza NP antibody, examined by light microscopy, and scored in a blinded fashion by a pathologist according to common guidelines (7). Frequency and severity of lesions in the bronchi/bronchioles, alveoli, and nasal turbinates were incorporated into the total score. Monocytes/macrophages were stained with rabbit anti-human lysozyme polyclonal antibody (Dako).

Assessment of Pulmonary Inflammation and Vascular Permeability. Mouse bronchoalveolar lavage (BALF) samples were collected by washing the lungs three times via catheter with 0.5 mL PBS containing 2mM EDTA (1.5mL total). After centrifugation, total infiltrating cells and neutrophils were counted. Supernatants were stored at -80°C. Proinflammatory cytokines and chemokines were measured by MILLIPLEX mouse magnetic bead assay (Millipore). Vascular permeability was assessed by assaying high molecular–

weight proteins and albumin-bound Evans blue dye in BALF as a measure of pulmonary extravasation (8). High molecular weight proteins were assayed in BALF by using Coomassie (Bradford) protein reagent (Thermo Scientific). To measure extravasation of albumin, Evans blue dye (Sigma) was injected retroorbitally under isoflurane anesthesia. After 4h, mice were euthanized and lungs were perfused, weighed, and incubated in formamide for 48 h at 65°C. The lung permeability index of each mouse was calculated by normalizing the absorbance of formamide at 620 nm to the absorbance of serum.

Ferret cytokine mRNA Analysis. RNAlater-preserved ferret tissues were homogenized, and total RNA was extracted using the RNeasy Mini Kit (Qiagen). IFN-α, TNF-α, IFN-γ, IL-6, IL-8, CXCL9, CXCL10, CXCL11 mRNA levels were analyzed by semiquantitative real-time PCR analysis on a 7500 Fast Real Time PCR system (Applied Biosystems) as described previously (9). Briefly, 10 ng of RNA and specific primers were mixed with the QuantiTect SYBR green RT-PCR master mix (Qiagen), following the manufacturer's instructions. Specific primers for the following ferret housekeeping gene and cytokines were previously described: GAPDH, IFN-α, TNF-α, IFN-γ and IL-6 (9), IL-8, CXCL9, CXCL10 and CXCL11 (10). Samples were analyzed in triplicate. After normalization to GAPDH, the fold change ratio of expression in virus-infected to control samples was calculated for each gene by using the ΔΔCt method and expressed as $2^{-\Delta\Delta Ct}$.

Antibody Titration. Blood was collected from ferrets 3 weeks after virus inoculation and centrifuged; anti-pH1N1 antibody was measured in the serum by hemagglutination inhibition (HI) assay. Briefly, 2-fold serial dilutions of receptor destroying enzyme (RDE)-treated sera were incubated with pH1N1 virus for 1 h to allow antigen-antibody binding. 0.5% turkey red blood cells were then added. The HI titer was determined as the reciprocal of the highest serum dilution that completely inhibited hemagglutination.

Enzyme linked-immunosorbent assay (ELISA) was performed as follows to measure the antibody levels. High-affinity plates were incubated overnight with 1 HA unit per well of sucrose-purified virus (A/Tennessee/1-560/2009 strain) at 4°C. PBS alone was used in negative control wells. Plates were washed with PBS containing 0.05% Tween 20 and incubated with 3% BSA for 2 h. Serially diluted sera were added to the wells and incubated for 3 h. After washing, horseradish peroxidase-linked goat anti-ferret IgG polyclonal antibody (Abcam) was added for 1 h. Finally, tetramethylbenzidine substrate (ThermoScientific) was added as chromogen. Optical density (O.D.) was read at 450nm on a microplate reader and corrected (C.O.D.) by subtraction of the corresponding negative control wells.

SI Appendix References

1. Krunkosky TM, Martin LD, Fischer BM, Voynow JA, & Adler KB (2003) Effects of TNFalpha on expression of ICAM-1 in human airway epithelial cells in vitro: oxidant-mediated pathways and transcription factors. *Free Radic Biol Med* 35(9):1158-1167.
2. Hoffmann E, Neumann G, Kawaoka Y, Hobom G, & Webster RG (2000) A DNA transfection system for generation of influenza A virus from eight plasmids. *Proc Natl Acad Sci U S A* 97(11):6108-6113.
3. Reed ML*, et al.* (2010) The pH of activation of the hemagglutinin protein regulates H5N1 influenza virus pathogenicity and transmissibility in ducks. *J Virol* 84(3):1527-1535.
4. Galloway SE, Reed ML, Russell CJ, & Steinhauer DA (2013) Influenza HA subtypes demonstrate divergent phenotypes for cleavage activation and pH of fusion: implications for host range and adaptation. *PLoS Pathog* 9(2):e1003151.
5. Reed ML*, et al.* (2009) Amino acid residues in the fusion peptide pocket regulate the pH of activation of the H5N1 influenza virus hemagglutinin protein. *J Virol* 83(8):3568-3580.
6. Reed LJ & Muench H (1938) A simple method of estimating fifty per cent endpoints. *Am J Hyg* 27(3):493-497.
7. Ward JM & Rehg JE (2014) Rodent immunohistochemistry: pitfalls and troubleshooting. *Vet Pathol* 51(1):88-101.
8. Saria A & Lundberg JM (1983) Evans blue fluorescence: quantitative and morphological evaluation of vascular permeability in animal tissues. *J Neurosci Methods* 8(1):41-49.
9. Svitek N & von Messling V (2007) Early cytokine mRNA expression profiles predict Morbillivirus disease outcome in ferrets. *Virology* 362(2):404-410.
10. Maines TR*, et al.* (2012) Local innate immune responses and influenza virus transmission and virulence in ferrets. *J Infect Dis* 205(3):474-485.
11. Daniels RS*, et al.* (1985) Fusion mutants of the influenza virus hemagglutinin glycoprotein. *Cell* 40(2):431-439.
12. Thoennes S*, et al.* (2008) Analysis of residues near the fusion peptide in the influenza hemagglutinin structure for roles in triggering membrane fusion. *Virology* 370(2):403-414.
13. Xu R & Wilson IA (2011) Structural characterization of an early fusion intermediate of influenza virus hemagglutinin. *J Virol* 85(10):5172-5182.

14. Gorman OT, Bean WJ, Kawaoka Y, & Webster RG (1990) Evolution of the nucleoprotein gene of influenza A virus. *J Virol* 64(4):1487-1497.

15. Wright SM, Kawaoka Y, Sharp GB, Senne DA, & Webster RG (1992) Interspecies transmission and reassortment of influenza A viruses in pigs and turkeys in the United States. *Am J Epidemiol* 136(4):488-497.

16. Hinshaw VS, Bean WJ, Jr., Webster RG, & Easterday BC (1978) The prevalence of influenza viruses in swine and the antigenic and genetic relatedness of influenza viruses from man and swine. *Virology* 84(1):51-62.

17. Krumbholz A*, et al.* (2014) Origin of the European avian-like swine influenza viruses. *J Gen Virol* 95(Pt 11):2372-2376.

18. Guan Y*, et al.* (1996) Emergence of avian H1N1 influenza viruses in pigs in China. *J Virol* 70(11):8041-8046.

19. Campitelli L*, et al.* (1997) Continued evolution of H1N1 and H3N2 influenza viruses in pigs in Italy. *Virology* 232(2):310-318.

20. Kocer ZA, Krauss S, Stallknecht DE, Rehg JE, & Webster RG (2012) The potential of avian H1N1 influenza A viruses to replicate and cause disease in mammalian models. *PLoS One* 7(7):e41609.

21. Webby RJ, Rossow K, Erickson G, Sims Y, & Webster R (2004) Multiple lineages of antigenically and genetically diverse influenza A virus co-circulate in the United States swine population. *Virus Res* 103(1-2):67-73.

22. Barman S*, et al.* (2012) Pathogenicity and transmissibility of North American triple reassortant swine influenza A viruses in ferrets. *PLoS Pathog* 8(7):e1002791.

23. Garten RJ*, et al.* (2009) Antigenic and genetic characteristics of swine-origin 2009 A(H1N1) influenza viruses circulating in humans. *Science* 325(5937):197-201.

24. Oshansky CM*, et al.* (2014) Mucosal immune responses predict clinical outcomes during influenza infection independently of age and viral load. *Am J Respir Crit Care Med* 189(4):449-462.

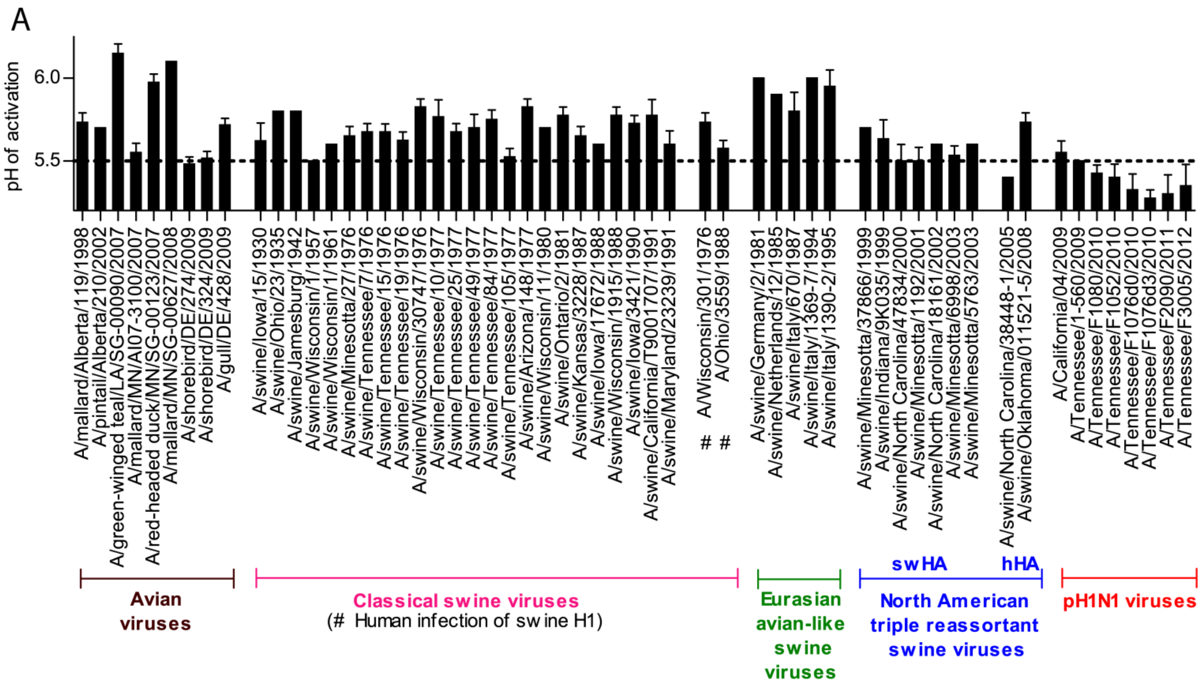

Figure S1. HA activation pH values for pH1N1 influenza viruses and potential H1 swine precursors. The panel of viruses included representatives of the classical swine lineage, Eurasian swine lineage, and North American triple reassortant lineage with swine-like (swHA) or human-like (hHA) HA, and early and later human pandemic pH1N1 virus isolates. Avian H1N1 viruses are also included as a point of reference. (*A*) For comparison, the pH of HA activation of the viruses was determined by using a syncytia assay in Vero cells. Data are the mean ± SD from 2-3 independent experiments with duplicates. The dotted line shows the activation pH of the early pH1N1 viruses (pH 5.5). # indicates human infection with swine H1 virus. (*B*) Maximum likelihood phylogenetic tree based on amino acid sequences inferred from the HA genes of selected H1 influenza viruses. The viruses were selected to represent the classical, Eurasian, and North American triple reassortant swine lineages. Two viruses of the classical swine lineage were isolated from infected humans (#). The human viruses A/Puerto Rico/8/1934 and A/Brisbane/59/2007 (seasonal H1) were added as references. HA amino acid sequences were aligned by using ClustalW Multiple Alignment software (Table S1). The phylogenetic tree was computed by using Mega5.1 software.

B
A/swine/Iowa/15/1930 (H1N1)
A/swine/Jamesburg/1942 (H1N1)
A/swine/Ohio/23/1935 (H1N1)
A/swine/Wisconsin/1/1957 (H1N1)
A/swine/Wisconsin/1/1961 (H1N1)
A/swine/Tennessee/105/1977 (H1N1)
A/swine/Arizona/148/1977 (H1N1)
A/swine/Minnesota/27/1976 (H1N1)
A/swine/Tennessee/49/1977 (H1N1)
A/swine/Tennessee/15/1976 (H1N1)
A/swine/Tennessee/25/1977 (H1N1)
A/swine/Tennessee/7/1976 (H1N1)
A/swine/Tennessee/19/1976 (H1N1)
A/Wisconsin/301/1976 (H1N1) #
A/swine/Wisconsin/30747/1976 (H1N1)
A/swine/Tennessee/10/1977 (H1N1)
A/swine/Tennessee/84/1977 (H1N1)
A/swine/Ontario/2/1981 (H1N1)
A/swine/Wisconsin/11/1980 (H1N1)
A/swine/Kansas/3228/1987 (H1N1)
A/Ohio/3559/1988 (H1N1) #
A/swine/Iowa/3421/1990 (H1N1)
A/swine/Wisconsin/1915/1988 (H1N1)
A/swine/Iowa/17672/1988 (H1N1)
A/swine/California/T9001707/1991 (H1N1)
A/swine/Maryland/23239/1991 (H1N1)
A/swine/North Carolina/47834/2000 (H1N1)
A/swine/Minnesota/6998/2003 (H1N1)
A/swine/Minnesota/37866/1999 (H1N1)
A/swine/Indiana/9K035/1999 (H1N2)
A/swine/Minnesota/5763/2003 (H1N2)
A/swine/Minnesota/1192/2001 (H1N2)
A/swine/North Carolina/18161/2002 (H1N1)
A/California/04/2009 (H1N1)
A/Tennessee/1-560/2009 (H1N1)
A/Tennessee/F3005/2012 (H1N1)
A/Tennessee/F2090/2011 (H1N1)
A/Tennessee/F1080/2010 (H1N1)
A/Tennessee/F1076d3/2010 (H1N1)
A/Tennessee/F1076d0/2010 (H1N1)
A/Tennessee/F1052/2010 (H1N1)
swHA
A/swine/North Carolina/38448-1/2005 (H1N1)
A/swine/Oklahoma/011521-5/2008 (H1N2)
hHA
A/Brisbane/59/2007 (H1N1)
A/Puerto Rico/8/1934 (H1N1)
A/swine/Italy/1369-7/1994 (H1N1)
A/swine/Italy/1390-2/1995 (H1N1)
A/swine/Italy/670/1987 (H1N1)
A/swine/Germany/2/1981 (H1N1)
A/swine/Netherlands/12/1985 (H1N1)
A/pintail/Alberta/210/2002(H1N1)
A/green-winged teal/Louisiana/Sg-00090/2007(H1N1)
A/red-headed duck/Minnesota/Sg-00123/2007(H1N1)
A/mallard/Minnesota/AI07-3100/2007(H1N1)
A/mallard/Minnesota/Sg-00627/2008(H1N1)
A/mallard/Alberta/119/1998 (H1N1)
A/gull/Delaware/428/2009(H1N1)
A/shorebird/Delaware/274/2009(H1N1)
A/shorebird/Delaware/324/2009(H1N1)
0.02
Classical swine H1 viruses
North American triple reassortant swine H1 viruses
pH1N1 viruses
Eurasian avian like swine H1 viruses
Avian H1 viruses
sporadic human infection with swine H1
Classical swine lineage
Eurasian avian-like swine lineage
Avian lineage

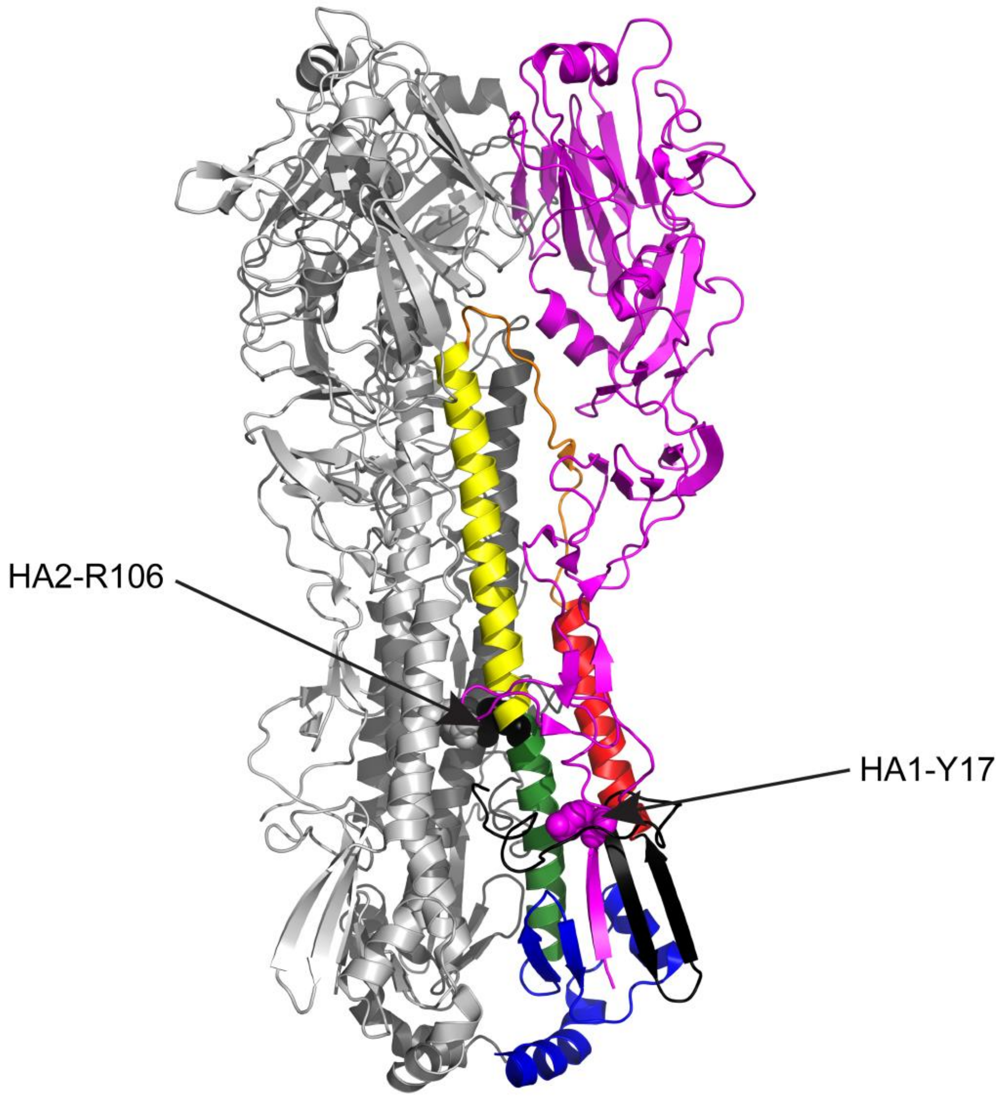

Figure S2. Locations of mutations in the pH1N1 HA protein. In the crystal structure of the HA protein of A/CA/04/09 (PDB entry 3UBE), two protomers are shaded gray and a third is color coded as follows: HA1 (magenta), fusion peptide (black), helix A (red), loop B (orange), helix C (yellow), helix D (green), and membrane-proximal region (blue). HA1 residue 17 is located in the fusion peptide pocket where the hydroxyl group of tyrosine in WT forms a hydrogen bond to the fusion peptide. An HA1-Y17H mutation breaks this hydrogen bond, increasing the HA activation pH (11, 12). HA2 residue 106 is positioned in the core of the coiled coil where the three positively-charged WT arginine residues in the trimer interface exert repulsive force, helping to destabilize the core which, once triggered, forms a hinge at this location. An HA2-R106K mutation decreases the electrostatic repulsion in the core, thereby stabilizing the HA protein and decreasing its activation pH (13). H3 numbering is used. Residues HA1-17 and HA2-106 are residues 24 and 450 with respect to the initiating methionine in the H1N1 HA protein (H1 numbering).

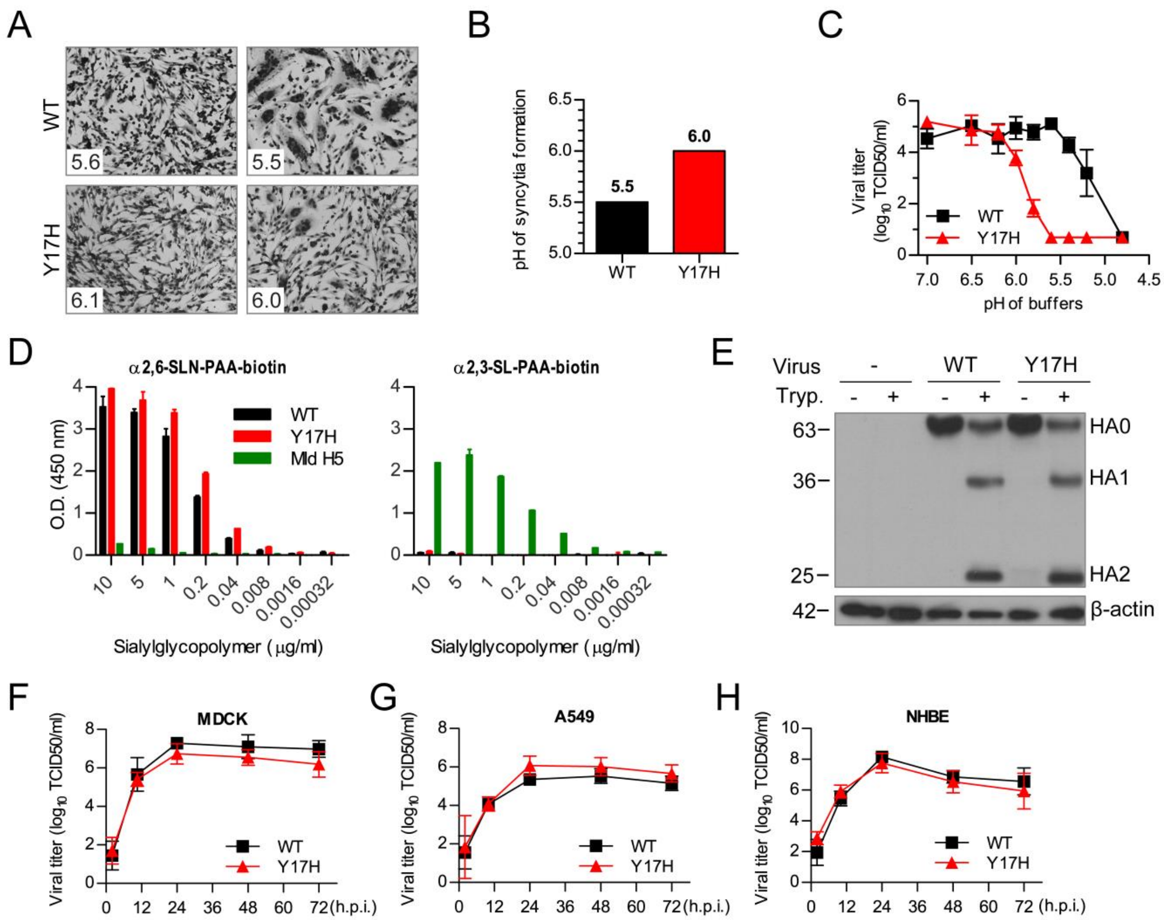

Figure S3. *In vitro* properties of pH1N1 WT and destabilized HA1-Y17H mutant. (*A*) Syncytia formation of BHK cells infected with WT and Y17H viruses. At left, normal monolayer is shown; at right, syncytia are observed after low pH treatment. (*B*) Mean HA activation pH measured by syncytia formation in BHK and Vero cells. (*C*) Acid inactivation of WT and Y17H virus. Mean (± SD) of one representative experiment performed in triplicate is shown. (*D*) HA receptor-binding specificity for α2,3- (avian-like) vs. α2,6-linked (human-like) glycans as determined by solid-phase assay. Optical density (O.D.) values are the mean (± SD) of one representative experiment performed in duplicate. When combining data from both experiments, there was no significant difference in receptor binding for WT and Y17H. A recombinant avian-like virus expressing H5 HA (Mld H5) was included as a control. (*E*) Western blot showing comparable HA expression and cleavage in infected Vero cells without (–) and with (+) exogenous TPCK-trypsin (Tryp.). (*F-H*) Virus replication in MDCK (*F*), A549 (*G*) and NHBE (*H*) cells. Virus titers are the mean (± SD) of 2-3 experiments. h.p.i., hours post-inoculation.

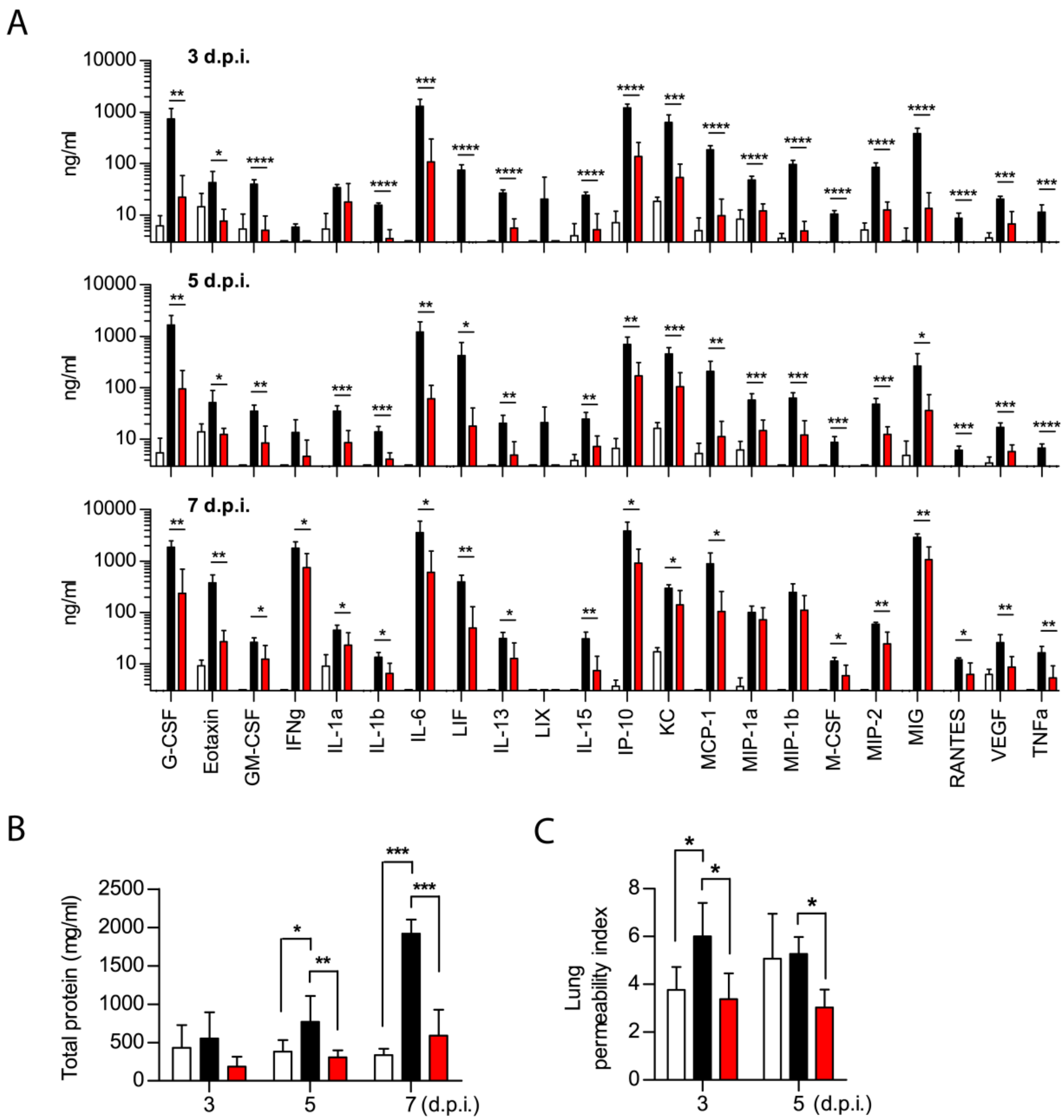

Figure S4. Inflammatory responses in the lungs of DBA/2J mice. Mice were inoculated as in Fig. 2. (*A*) Mean (± SD) concentration of proinflammatory cytokines and chemokines (released by infiltrating cells) in BALF supernatant at 3, 5, and 7 d.p.i. in of 5-6 mice. (*B*) Mean (± SD) concentration of total protein in BALF at 3, 5, and 7 d.p.i. in groups of 5-6 mice. (*C*) Mean (± SD) lung permeability at 3 and 5 d.p.i. as indicated by extravasation of Evans blue dye–stained albumin into the airspaces (n=5). One-way ANOVA at each time point was followed by Tukey test (*B*,*C*) or Student test (*A*; WT vs. Y17H only): *, $p<0.05$; **, $p<0.01$; ***, $p<0.001$; ****, $p<0.0001$.

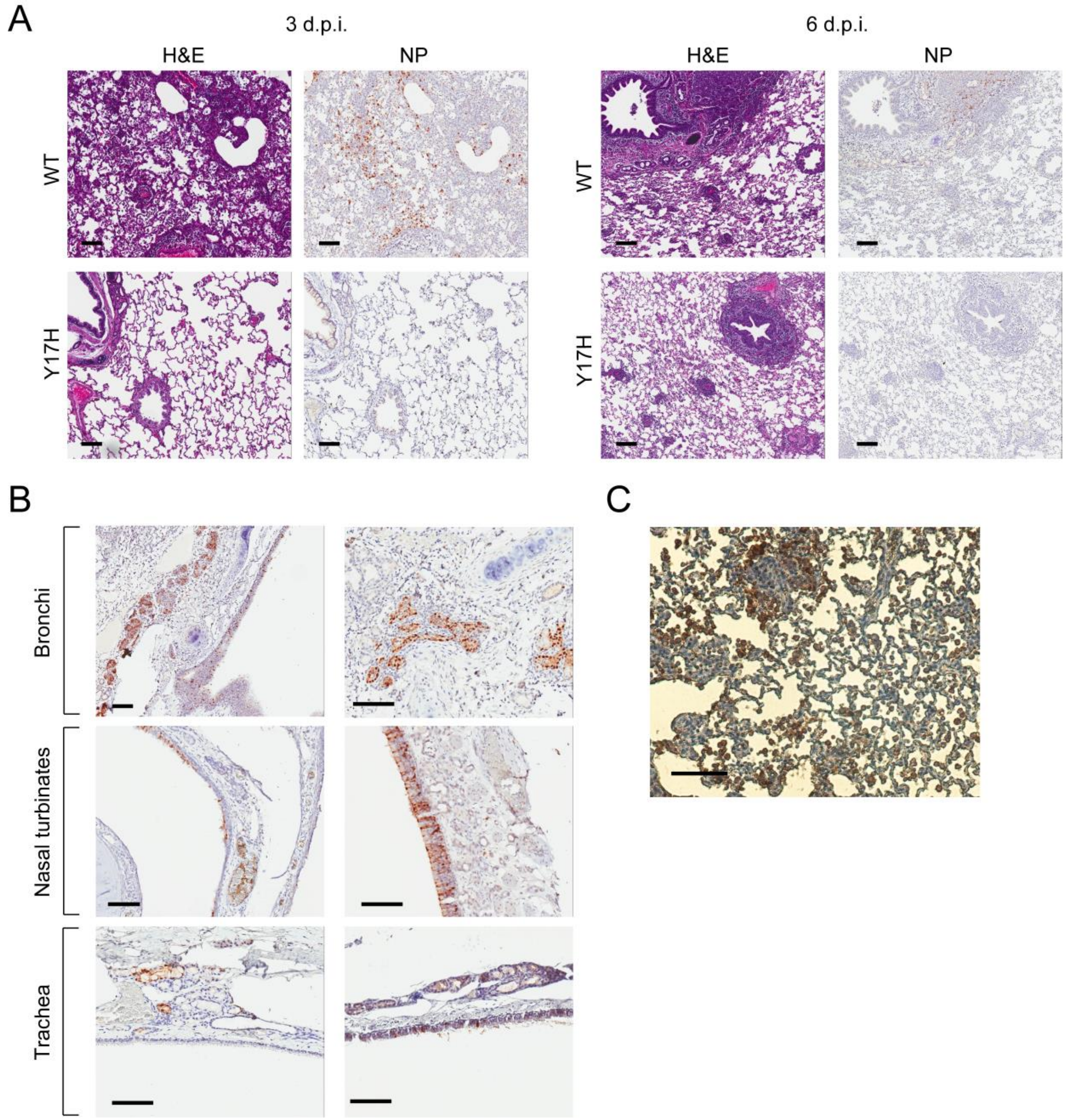

Figure S5. Histology and immunohistochemistry findings in infected ferrets. (*A*) Representative features of lower respiratory tract tissues infected with wild-type (WT) or Y17H–HA mutant (Y17H) pH1N1 virus. Lesions include alveolar septal thickening, infiltration of bronchial and bronchiolar lumens and alveoli with inflammatory cells, pneumocyte hyperplasia, and bronchial and bronchiolar epithelial necrosis producing cell debris in the lumens. The control group showed no lesions (not shown). d.p.i., days post-inoculation; H&E, hematoxylin and eosin; NP, polyclonal anti-NP staining (*B*) Representative features of bronchi, nasal turbinates, and trachea infected with WT pH1N1 virus showing infection in the epithelium and the submucosal glands. Y17H–HA mutant virus showed similar tissue tropism (not shown). (*C*) Lysozyme staining shows infiltration of alveoli with monocytes and macrophages during infection with WT virus. Findings were similar after Y17H virus infection (not shown). Scale bar, 100µm.

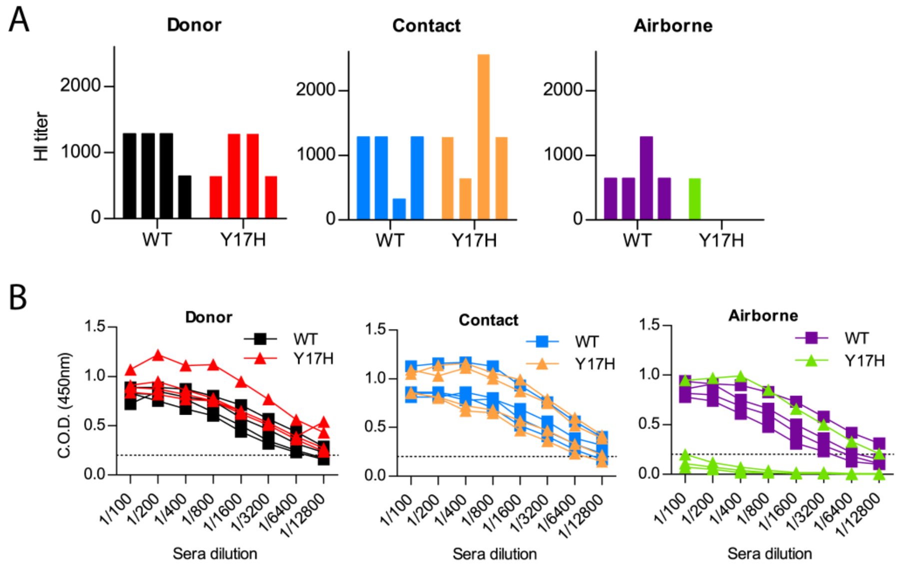

Figure S6. Serum antibody levels in ferrets infected with WT or Y17H-mutant (unstable HA) pH1N1 viruses. Four donor ferrets (black and red bars) were inoculated intranasally with 10^6 $TCID_{50}$ of WT (black, blue, and purple) or Y17H–HA mutant pH1N1 (red, orange, and green). The following day, 1 naïve ferret was introduced into each cage (contact ferret) or into an adjacent cage (airborne-transmission ferret, purple, and green bars). Serum was collected from all animals 3 weeks after donor inoculation. Neutralizing antibody titers were measured by hemagglutination inhibition (HI) assay (*A*) and total IgG antibody levels were measured by ELISA (*B*).

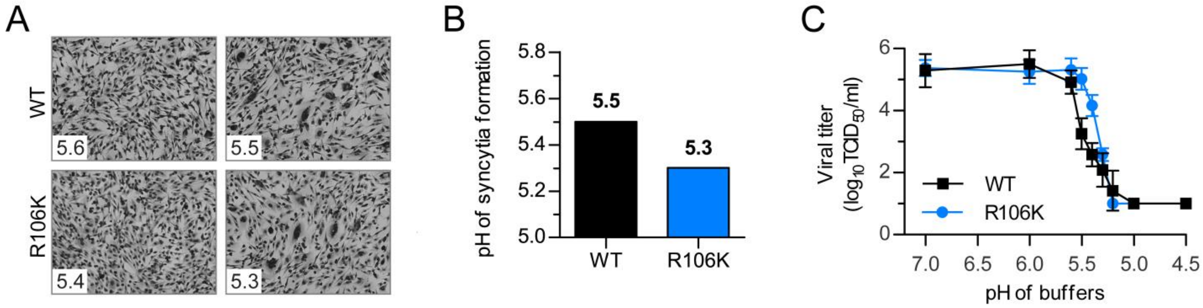

Figure S7. *In vitro* properties of pH1N1 containing an HA2-R106K mutation. The mutant virus was generated by reverse genetics. (*A*) Syncytia formation of BHK cells infected with WT and R106K viruses. At left, normal monolayer is shown; at right, syncytia are observed after low pH treatment. (*B*) Mean HA activation pH measured by syncytia formation in BHK cells. (*C*) Acid inactivation of WT (black) and R106K (blue) viruses. Mean (± SD) correspond to two experiments with duplicate samples.

Table S1. Influenza viruses used in the study.

Strain[a]	Subtype	GenBank accession number	Reference
A/swine/Iowa/15/1930	H1N1	EU139823	(14)
A/Puerto Rico/8/1934	H1N1	CY121109	NA
A/swine/Jamesburg/1942	H1N1	CY026427.1	This report
A/swine/Ohio/23/1935	H1N1	CY027291.1	This report
A/swine/Wisconsin/1/1957	H1N1	CY026283.1	This report
A/swine/Wisconsin/1/1961	H1N1	CY032213.1	This report
A/swine/Minnesota/27/1976	H1N1	CY022357.1	(15)
A/swine/Tennessee/7/1976	H1N1	CY022037.1	(16)
A/swine/Tennessee/15/1976	H1N1	CY022045.1	(16)
A/swine/Tennessee/19/1976	H1N1	CY022061.1	(16)
A/Wisconsin/301/1976	H1N1	CY026139.1	(16)
A/swine/Wisconsin/30747/1976	H1N1	CY028187.1	(15)
A/swine/Tennessee/10/1977	H1N1	CY022269.1	(16)
A/swine/Tennessee/25/1977	H1N1	CY009916.1	(16)
A/swine/Tennessee/49/1977	H1N1	CY022133.1	(16)
A/swine/Tennessee/84/1977	H1N1	CY024954.1	(16)
A/swine/Tennessee/105/1977	H1N1	CY026475.1	(16)
A/swine/Arizona/148/1977	H1N1	CY025002.1	This report
A/swine/Wisconsin/11/1980	H1N1	CY022421.1	(15)
A/swine/Germany/2/1981	H1N1	KJ889356.1	(17)
A/swine/Ontario/2/1981	H1N1	CY026435.1	This report
A/swine/Netherlands/12/1985	H1N1	AF091317.1	(18)
A/swine/Italy/670/1987	H1N1	CY025253.1	(19)
A/swine/Kansas/3228/1987	H1N1	CY022469.1	(15)
A/swine/Iowa/17672/1988	H1N1	CY022333.1	This report
A/Ohio/3559/1988	H1N1	CY024925.1	This report[b]
A/swine/Wisconsin/1915/1988	H1N1	CY022429.1	(15)
A/swine/Iowa/3421/1990	H1N1	CY096875.1	(15)
A/swine/California/T9001707/1991	H1N1	CY028780.1	(15)
A/swine/Maryland/23239/1991	H1N1	CY022477.1	(15)
A/swine/Italy/1369-7/1994	H1N1	CY098500.1	(19)
A/swine/Italy/1390-2/1995	H1N1	Not submitted[c]	(19)
A/mallard/Alberta/119/1998	H1N1	KF424178.1	(20)
A/swine/Minnesota/37866/1999	H1N1	EU139827.1	(21)
A/swine/Indiana/9K035/1999	H1N2	AF250124.1	(22)
A/swine/North Carolina/47834/2000	H1N1	CY098476.1	(22)
A/swine/Minnesota/1192/2001	H1N2	CY098465-72	(22)
A/pintail/Alberta/210/2002	H1N1	KF424114.1	(20)
A/swine/North Carolina/18161/2002	H1N1	CY098513-20	(21)
A/swine/Minnesota/6998/2003	H1N1	CY098481-88	(22)
A/swine/Minnesota/5763/2003	H1N2	CY098489-96	(22)
A/swine/North Carolina/38448-1/2005	H1N1	CY098506-12	(22)
A/Brisbane/59/2007	H1N1	CY030230.1	NA
A/green-winged teal/Louisiana/SG-00090/2007	H1N1	KF424090.1	(20)
A/mallard/Minnesota/AI07-3100/2007	H1N1	KF424018	(20)
A/redheaded duck/Minnesota/SG-00123/2007	H1N1	KF424194.1	(20)
A/mallard/Minnesota/SG-00627/2008	H1N1	KF424058.1	(20)
A/swine/Oklahoma/011521-5/2008	H1N2	CY045647.1	(22)
A/California/04/2009	pH1N1	FJ966082.1	(23)
A/Tennessee/1-560/2009	pH1N1	CY040457.1	This report
A/gull/Delaware/428/2009	H1N1	KF424026.1	(20)
A/shorebird/Delaware/274/2009	H1N1	KF424066.1	(20)

A/shorebird/Delaware/324/2009	H1N1	KF424082.1	(20)
A/Tennessee/F1052/2010	pH1N1	Not submitted[c]	(24)
A/Tennessee/F1076d0/2010	pH1N1	Not submitted[c]	(24)
A/Tennessee/F1076d3/2010	pH1N1	Not submitted[c]	(24)
A/Tennessee/F1080/2010	pH1N1	CY167780.1	(24)
A/Tennessee/F2090/2011	pH1N1	CY167748.1	(24)
A/Tennessee/F3005/2012	pH1N1	Not submitted[c]	(24)

[a] Swine viruses were isolated during epidemiologic surveys in pig farms. Human pH1N1 viruses were isolated during a human cohort study. A/Puerto Rico/8/1934 and A/Brisbane/59/2007 were used only as references for phylogenetic analysis. All other viruses were obtained from the St. Jude repository.

[b] This virus was isolated from a human after an outbreak of swine influenza in Fort Dix, NJ in 1976.

[c] Viruses were sequenced for this study by the Hartwell Center for Bioinformatics and Biotechnology at St. Jude.

NA, not applicable.

Table S2. Extent of infection of respiratory tissues detected by immunohistochemical staining for viral NP antigen in DBA/2J mice and ferrets inoculated with WT or HA1-Y17H–mutant pH1N1 virus.

		3 d.p.i.		5 d.p.i.	
		WT	Y17H	WT	Y17H
DBA2/J mice	Bronchioles (% NP+)[a]	43%	7.3%	46.7%	8.3%
	Alveoli (Total no. NP+ cells)[b]	203	11	265	119
	Trachea (Total no. NP+ cells)[b]	2	31	8	97
	Nasal turbinates (Total no. NP+ cells)[b]	12	0	54	12
		3 d.p.i.		**6 d.p.i.**	
		WT	**Y17H**	**WT**	**Y17H**
ferrets	Bronchi (Total no. NP+ cells)[c]	524	19	0	0
	Submucosa (Total no. NP+ cells)[c]	3331	86	134	120
	Bronchioles (Total no. NP+ cells)[c]	352	66	28	84
	Alveoli (Total no. NP+ cells)[c]	854	33	62	112
	Trachea (Total no. NP+ cells)[d]	6	0	0	0
	Rostral nasal turbinates (Total no. NP+ cells)[e]	19	87	7	0
	Middle nasal turbinates (Total no. NP+ cells)[e]	1414	3651	38	267
	Caudal nasal turbinates (Total no. NP+ cells)[e]	3722	91	245	297

Mice and ferrets were inoculated intranasally with 750 PFU and 10^6 $TCID_{50}$ PFU virus, respectively. Tissues were collected at the reported days post-inoculation (d.p.i.). Slides were stained for immunohistochemistry with an anti–influenza virus nucleoprotein (NP) antibody. All control tissues (PBS-inoculated) were negative.

[a] The mean percentage in 3 mice.

[b] The mean total number in 3 mice.

[c] NP-positive cells were counted in one tissue section from each lung lobe and are reported as the mean value in 3 ferrets.

[d] NP+ cells were counted in one cross section and one longitudinal section of the trachea.

[e] The rostral, middle, and caudal divisions of the nasal turbinates comprise 4, 3, and 4 sections, respectively.

Table S3. Genotypes of pH1N1 viruses isolated from ferrets after transmission.

H1 numbering	H3 numbering	Inoculum	Cage #5				Cage #6				Cage #7					Cage #8								
			Donor		Contact		Donor		Contact		Donor			Contact		Donor			Contact			Airborne		
			3	5	7	9	3	5	5	9	1	3	5	7	9	1	3	5	5	7	9	7	9	11
24	HA1-17	H				Y							Y	Y	Y					Y	Y	Y	Y	Y
36	HA1-29	V		I		I	A			I	E	E	E	E										
100	HA1-91	S				P																		
103	HA1-93	D																					G	
207	HA1-193	S																						N
214	HA1-200	A				T																		
220	HA1-206	T				S																		
239	HA1-225	D				G																		
305	HA1-290	T	A	A			A	A I	A	A						A	A	A	A	A	A			
306	HA1-291	S	N I	N I		N					N	N				N	N	N	N	N	N			
338	HA1-323	V									I													
369	HA2-25	H			Y	Y					Y	Y	Y											
387	HA2-43	N								K														
399	HA2-55	V				F		I																
442	HA2-98	L								M														
446	HA2-102	L											V											
450	HA2-106	R					K	K	K	K	K	K	K			K	K	K	K	K	K	K	K	K
453	HA2-109	D					N																	
528	HA2-184	Y				C					C													

0 5 10 30 50 75 95 100

Proportion of variants (%)

The HA, NA, and M segments of all isolated viruses were sequenced in all virus-containing nasal washes collected at all time points. No substitutions were found in NA or M proteins. No amino changes were found in the WT group.

In the Y17H group, the HA gene of viruses was sequenced by Sanger and next generation sequencing (if enough sample was available). The proportion of variants from next generation sequencing is reported using both H1 and H3 numbering. For cage 5 and 6 donors on day 1 and cage 5 contact recipient on day 5, sufficient sample was not available for next generation sequencing but Sanger sequencing showed no difference from the inoculated virus (HA1-H17 and HA2-R106).